ACS chemical biology

Articles

pubs.acs.org/acschemicalbiology

Synthesis and Biological Evaluation of Optimized Inhibitors of the Mitotic Kinesin Kif18A

Joachim Braun,[†,§] Martin M. Möckel,[‡,§] Tobias Strittmatter,[†] Andreas Marx,[†] Ulrich Groth,[†] and Thomas U. Mayer*[,‡]

[†]Department of Chemistry and Konstanz Research School Chemical-Biology (KoRS-CB), University of Konstanz, Universitätsstr. 10, 78467 Konstanz, Germany

[‡]Department of Biology and Konstanz Research School Chemical-Biology (KoRS-CB), University of Konstanz, Universitätsstr. 10, 78467 Konstanz, Germany

Supporting Information

ABSTRACT: The mitotic spindle, a highly dynamic structure composed of microtubules, mediates the segregation of the previously duplicated genome into the two nascent daughter cells. Errors in this process contribute to pathology including tumor formation. Key for the shape and function of the mitotic spindle are kinesins, molecular motor proteins that convert chemical energy into mechanical work. Due to their fast mode of action, small molecules are valuable tools to dissect the dynamic functions of kinesins during mitosis. In this study, we report the identification of optimized small molecule inhibitors of the mitotic kinesin Kif18A. Using BTB-1, the first identified Kif18A inhibitor, as a lead compound, we synthesized a collection of derivatives. We demonstrate that some of the synthesized derivatives potently inhibited the ATPase activity of Kif18A with a half maximal inhibitory concentration (IC_{50}) value in the low micromolar range. *In vitro* analysis of a panel of Kif18A-related kinesins revealed that the two most potent compounds show improved selectivity compared to BTB-1. Structure−activity relationship studies identified substituents mediating undesired inhibitory effects on microtubule polymerization. In summary, our study provides key insights into the mechanism of action of BTB-1 and its analogs, which will have a great impact on the further development of highly selective and bioactive Kif18A inhibitors. Since Kif18A is frequently overexpressed in solid tumors, such compounds are not only of great interest for basic research but also have the potential to open up new strategies for the treatment of human diseases.

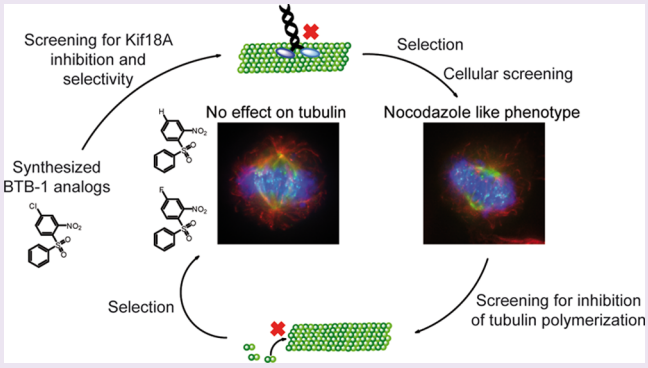

The genetic integrity of each organism is intimately tied to the faithful segregation of its genome during mitosis. In eukaryotes, this challenging task is mastered by the mitotic spindle, a bipolar structure composed of microtubule filaments.[1] The organization of the complex network of dynamic microtubules into the bipolar spindle shape and the process of chromosome segregation depends on the coordinated activities of kinesins.[2] Kinesins are molecular motor proteins that hydrolyze ATP and convert the released energy into mechanical work. Depending on the molecular architecture, kinesins typically perform the mechanical work in either of the three following forms: they move towards the highly dynamic plus end of microtubules, move towards the less dynamic minus end, or modulate microtubule dynamics.[3] The mitotic kinesin Kif18A is unique in that it integrates plus-end directed motility with the ability to affect microtubule dynamics.[4−9] Previous studies revealed that the function of Kif18A is essential for the accurate architecture of the mitotic spindle and proper alignment of chromosomes in mammalian cells, i.e. cells depleted of Kif18A by RNA interference (RNA_i) display elongated spindles with hyperstable microtubules and the majority of chromosomes scattered throughout the spindle.[4,8] Notably, multiple cancer types display elevated Kif18A levels, suggesting that its function might be beneficial for the survival and development of these cells.[10−12] Previously, we reported the identification of BTB-1 (**1**, Figure 1A), the first small molecule inhibitor of Kif18A.[13] **1** reversibly inhibited the microtubule-stimulated ATPase activity of Kif18A with a half maximal inhibitory concentration (IC_{50}) of 1.7 μM. Treatment of HeLa-cells with **1** caused an increase in the percentage of cells that were in mitosis indicative of **1** being bioactive in tissue culture cells. However, in contrast to the depletion of Kif18A, treatment with high concentrations of **1** did not result in elongated spindles. On the basis of this phenotype, we speculated that Kif18A might not be the relevant binding partner of **1** in cells.

To better understand the mode of action of **1**, we synthesized a collection of 20 BTB-1 derivatives and analyzed

Received: October 1, 2014
Accepted: November 17, 2014

   dx.doi.org/10.1021/cb500789h | *ACS Chem. Biol.* XXXX, XXX, XXX−XXX

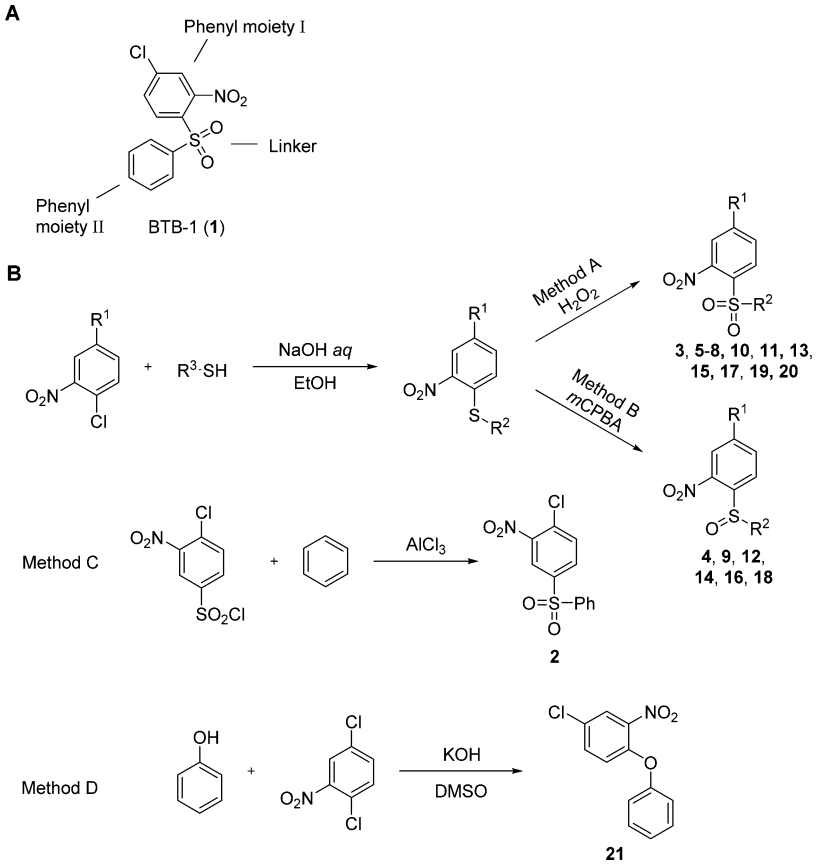

Figure 1. (A) Structure of BTB-1 (**1**). (B) Synthesis of BTB-1 analogs **2**–**21**.

these compounds in respect of their inhibitory activity against Kif18A, selectivity, and effect on cells. We identified novel inhibitors of Kif18A with an IC_{50} value in the low micromolar range. Structure–activity relationship (SAR) studies depicted substituents mediating undesired side effects on microtubule polymerization. Notably, one of the most potent Kif18A inhibitors identified in this study had no detectable inhibitory effect on microtubule polymerization. These insights into the mechanism of action of **1** and its derivatives provide essential guidelines for the future development and evaluation of highly potent and bioactive Kif18A inhibitors.

RESULTS AND DISCUSSION

Design of BTB-1 Derivatives and Their Synthesis. In order to get a better understanding of which structural motifs of **1** are necessary for its inhibitory activity against its target Kif18A and to potentially find more effective inhibitors, a subset of closely related analogs was synthesized (**2**–**21**). To this end, the unsymmetrically substituted diarylsulphone **1** was divided into three scaffolds: the two phenyl moieties I and II and a linker between them (Figure 1A). At position R^1, electron withdrawing substituents like fluorine, trifluoromethyl, and nitro groups were introduced to elucidate how altered electronegativity and sterical demand at this position impact the inhibitory activity and compound lipophilicity.

In addition, the requirement of the NO_2 substituent in the *ortho* position to the linker for the inhibitory activity was analyzed by shifting it in *meta* position. The second phenyl ring R^2 was exchanged to thiophene, and the aromatic system was expanded to naphthalene. Furthermore, various substituents (Cl, MeO, Me) were introduced in *para* position to the linker. Finally, the sulfone linker was changed to an ether or sulfoxide to analyze the effect of the geometry of the linker on the inhibition of Kif18A. The main reaction (Figure 1B) utilized to synthesize this series of BTB-1 derivatives was a nucleophilic aromatic substitution (S_NAr) under basic conditions to displace activated chloride at the aromatic core by aromatic thiols or thiolates as described for BTB-1.[13−15] The resulting sulfides were oxidized to the corresponding sulfons using H_2O_2 (Figure 1B, method A, Table 1) or to the racemic sulfoxides by *meta*-chloroperoxybenzoic acid (*m*CPBA; Figure 1B, method B, Table 1).

Compound **2** was synthesized according to Moore et al. by the $AlCl_3$ mediated reaction of benzol and the corresponding sulfonyl chloride in 46% yield (Figure 1B, method C).[16] The biphenyl ether **21** was synthesized using a S_NAr under basic conditions in DMSO in 96% yield (Figure 1B, method D).[17] All synthesized compounds were purified by column chromatography and/or successive recrystallization. The chemical identity of the molecules was confirmed by elementary and NMR analysis validating the described synthesis routes as robust and cost-efficient methods to assemble a small scale compound collection in a fast manner. For detailed synthetic procedures, see the Supporting Information.

Biochemical Evaluation of the Newly Synthesized BTB-1 Analogs. Kinesins hydrolyze ATP to walk along microtubules, and this activity can be easily quantified by an enzyme coupled assay (ECA) where ATP hydrolysis results in the oxidation of NADH and, thus, in a decrease in the absorbance at 340 nm (Figure 2A).[18] Using the recombinant motor domain of Kif18A fused to a His-Tag ($Kif18A^{MD}$), the conditions of the ECA were adjusted to obtain 50% inhibition

dx.doi.org/10.1021/cb500789h | ACS Chem. Biol. XXXX, XXX, XXX–XXX

Table 1. BTB-1 Analogs and Yields

no.	R^1 (scaffold I)	R^2 (scaffold II)	method	yield
1	Cl	Ph	A	74%[13]
2	1-chloro-2-nitro-4-(phenylsulfonyl) benzene		C	46%
3	NO_2	Ph	A	25%
4	NO_2	Ph	B	38%
5	F	Ph	A	12%
6	CF_3	Ph	A	26%
7	Cl	2-thiophene	A	68%
8	Cl	2-naphthalene	A	6%
9	Cl	2-naphthalene	B	66%
10	Cl	4-methylbenzene	A	7%
11	Cl	4-methoxybenzene	A	12%
12	Cl	4-methoxybenzene	B	72%
13	H	Ph	A	3%
14	H	Ph	B	13%
15	H	4-methoxybenzene	A	5%
16	H	4-methoxybenzene	B	2%
17	NO_2	4-methylbenzene	A	18%
18	NO_2	4-methylbenzene	B	20%
19	Cl	4-chlorobenzene	A	55%
20	NO_2	4-chlorobenzene	A	77%
21	4-chloro-2-nitro-1-phenoxybenzene		D	96%

at 5 μM **1** (Supporting Information). ATPase activity of $Kif18A^{MD}$ in the presence of DMSO was normalized to 100%. Of the tested 20 derivatives, five compounds (**3**, **5**, **6**, **7**, and **13**, Figure 2B) showed an inhibition of greater than 25% at a concentration of 5 μM, and these compounds were selected for further analysis.

Next, the IC_{50} values of these five compounds were determined using the ECA (Figure 2C, Supporting Information). While all compounds showed a dose dependent inhibition in the low micromolar range, none of them was more potent than **1** (1.7 ± 0.2 μM). **13** and **5** were the most potent inhibitors with IC_{50} values of 3.0 ± 0.2 μM and 4.8 ± 0.4 μM, respectively, indicating that the replacement of the halogene atom is tolerated. The introduction of more bulky substituents like NO_2 (**3**) or CF_3 (**6**) as well as the exchange of the phenyl moiety R^2 to a thiophene (**7**) resulted in reduced potency (IC_{50} values: (**3**) 10.2 ± 2.0 μM, (**6**) 10.3 ± 1.9 μM, and (**7**) 6.4 ± 0.9 μM).

ECA analysis of $Kif18A^{MD}$ activity in the absence of microtubules revealed that **13** and **5**—like **1**—had no inhibitory effect on the basal, microtubule-independent ATPase activity of Kif18A (Figures S1 and S2). Furthermore, ATP titration experiments indicate that **13** acts in an ATP-competitive manner (Figure S3). Thus, these data suggest that the identified derivatives—like **1** itself[13]—are ATP-competitive inhibitors that can only inhibit Kif18A when it is bound to microtubules. To analyze compound selectivity, the effects of the two most potent compounds **5** and **13** on the ATPase activity of other kinesins highly related to Kif18A were tested *in vitro*. To this end, ECA was performed in the presence of 100 μM **5** or **13** and His-tagged motor domains of the

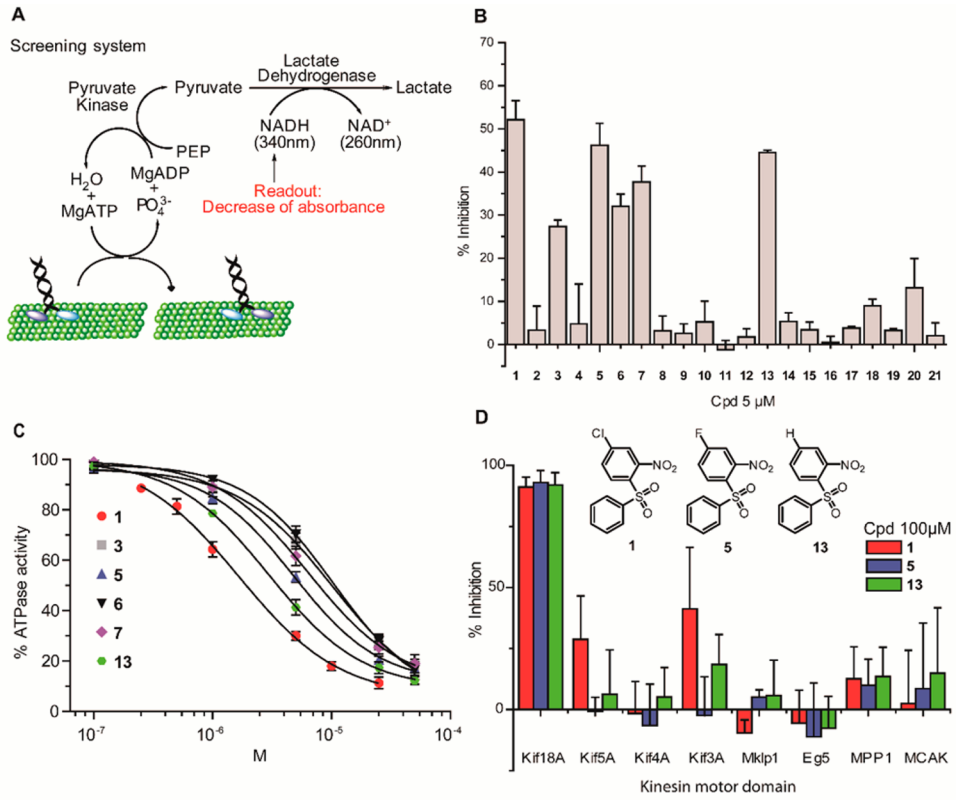

Figure 2. (A) Scheme of ECA used to quantify the ATPase activity of $Kif18A^{MD}$. (B) Quantification of the inhibitory activity of BTB-1 (**1**) and derivatives tested at 5 μM. Average of three independent experiments and standard deviations are shown. (C) Dose−response curves of **1**, **3**, **5**, **6**, **7**, and **13**. Average of three independent experiments and standard deviations are shown. (D) Quantification of the inhibitory activity of 100 μM **1**, **5**, and **13** on the ATPase activity of His-tagged motor-domain of the indicated mitotic kinesins. Average of three independent experiments and standard deviations are shown. For further details, see the Supporting Information.

dx.doi.org/10.1021/cb500789h | *ACS Chem. Biol.* XXXX, XXX, XXX−XXX

mitotic kinesins Kif3A, Kif4A, Kif5A, Mklp1, Eg5, MPP1, or MCAK. Compared to **1**, **5** and **13** showed reduced inhibitory activity towards Kif3A and Kif5A and comparable inhibitory activity towards the remaining tested kinesins, suggesting that the substitution of chloride with hydrogen and fluoride atoms increased compound selectivity.

Cellular Evaluation. Due to their fast and often reversible mode of action, small molecules are versatile tools to dissect dynamic cellular processes. To analyze if the identified novel Kif18A inhibitors are active in cells, we first analyzed the five most potent compounds **3**, **5**, **6**, **7**, and **13** for their cytotoxicity on HeLa cells.[19] Determination of the half maximal effective concentration (EC_{50} values) using an alamar blue assay (Figure 3, Supporting Information) revealed that compound **3** showed

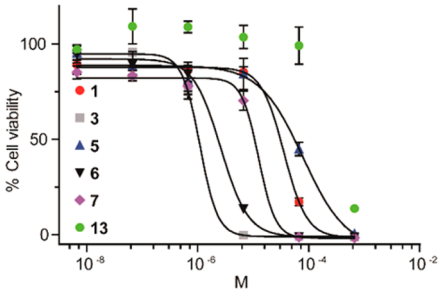

Figure 3. Quantification of compound cytotoxicity at indicated concentrations. Average of three independent experiments and standard deviations are shown. For further details, see the Supporting Information.

the highest cytotoxicity with 1.1 ± 0.3 μM followed by **6** with 2.6 ± 0.4 μM. **1** and **7** were less toxic with EC_{50} values of 35.8 ± 9.0 μM and 23.1 ± 7.3 μM, respectively. For **5**, the lowest cytotoxicity was observed with EC_{50} values above 50 μM, and **13** did not show a significant cytotoxicity at all.

Initial immunofluorescence analysis revealed that derivative **3** caused unspecific cytotoxic effects that affected both dividing and nondividing cells, and therefore, this compound was excluded from further microscopic studies. To analyze in detail the effect of **1** and derivatives **5**, **6**, and **13** on the architecture of the mitotic spindle, we used a previously established HeLa cell line that stably expresses green fluorescent protein (GFP) tagged Kif18A.[20] Cells synchronized in S-Phase were released for 9 h and then treated with the solvent control DMSO or 50 μM of **1** or derivatives **5**, **6**, and **13** (Figure 4A, Supporting Information). Thirty minutes after compound addition, cells were chemically fixed, and tubulin (red) and DNA (blue) structures were visualized by immunostaining and treatment with the dye Hoechst 33342, respectively. Microscopic analysis of mitotic spindles revealed that neither **5** nor **13** significantly affected spindle structures or alignment of chromosomes (Figure 4B). Furthermore, the accumulation of GFP-Kif18A at the plus ends of microtubules—which as shown previously depends on the motor activity of Kif18A[5−7]—was not affected by the treatment with **5** or **13**. This effect together with the observed normal spindle structures suggests that treatment with derivative **5** or **13** does not result in efficient Kif18A inhibition in cells. Consistent with previous reports,[13] analysis of HeLa cells treated with 50 μM **1** revealed severe defects in spindle morphology and chromosome alignment (Figure 4B). Similarly, multiple spindle poles, highly disorganized, and fragmented microtubule structures and no detectable alignment

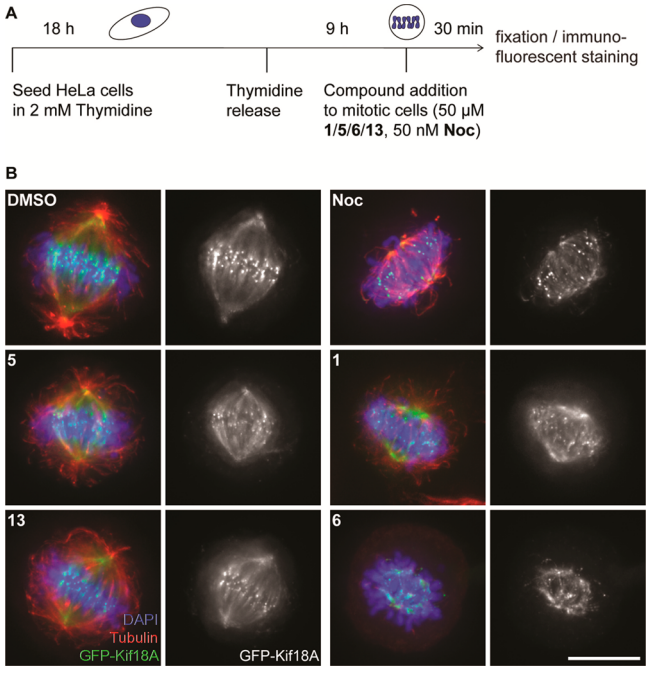

Figure 4. (A) Assay scheme for cell synchronization and compound treatment. First, cells were synchronized in S-Phase using thymidine. Nine hours after the release, cells were treated with DMSO, 50 nM Nocodazole (Noc), or 50 μM compounds **1**, **5**, **6**, and **13** followed by formalin fixation and immunostaining. (B) Representative immunofluorescence images of cells treated with DMSO, 50 nM Nocodazole (Noc), or 50 μM compounds **1**, **5**, **6**, and **13**. For each condition, merged images with DNA (blue), GFP-Kif18A (green), and microtubules (red) are shown on the left. GFP-Kif18A signal in gray is shown on the right (scale bar = 10 μm).

of chromosomes were observed in HeLa cells treated with 50 μM **6** (Figure 4B). Since Kif18A depletion results in elongated spindles with hyperstable microtubules,[4,8] the observed phenotypes tempted us to speculate that Kif18A is not the relevant binding partner of **1**[13] or **6** in cells.

Biochemical Evaluation on Tubulin Polymerization. The spindle phenotype induced by **6** was reminiscent of the phenotype caused by low doses of Nocodazole, a microtubule destabilizing compound (Figure 4B). To analyze if **6** as well as **1**, **3**, **5**, and **13** target microtubules, a turbidity-based *in vitro* microtubule polymerization assay was performed (Figure 5A, Supporting Information).[21,22] Microtubule polymerization efficiency in the presence of the solvent control DMSO was normalized to 100%. Notably, at 50 μM, all compounds had an inhibitory effect on microtubule polymerization, with **3** being the most potent molecule (Figure 5B).

Compound titration experiments revealed an IC_{50} value of 1.2 ± 0.1 μM for **3**, indicating that the high cytotoxicity of the compound might be due to its potent inhibitory effect on microtubule polymerization (Figure 5C). **1** and **6** had moderate effects on microtubule polymerization with IC_{50} values of 27.5 ± 3.3 μM and 9.2 ± 1.0 μM, respectively (Figure 5C). **13** inhibited microtubule polymerization with an IC_{50} value of 209.4 ± 37.3 μM, and **5** did not show any significant effect on the tubulin polymerization up to a concentration of 1 mM (Figure 5C). Thus, these studies revealed that the introduction of bulky substituents in phenyl moiety I at the *para* position to the linker drastically increased the undesired inhibitory effect on microtubule polymerization.

dx.doi.org/10.1021/cb500789h | *ACS Chem. Biol.* XXXX, XXX, XXX−XXX

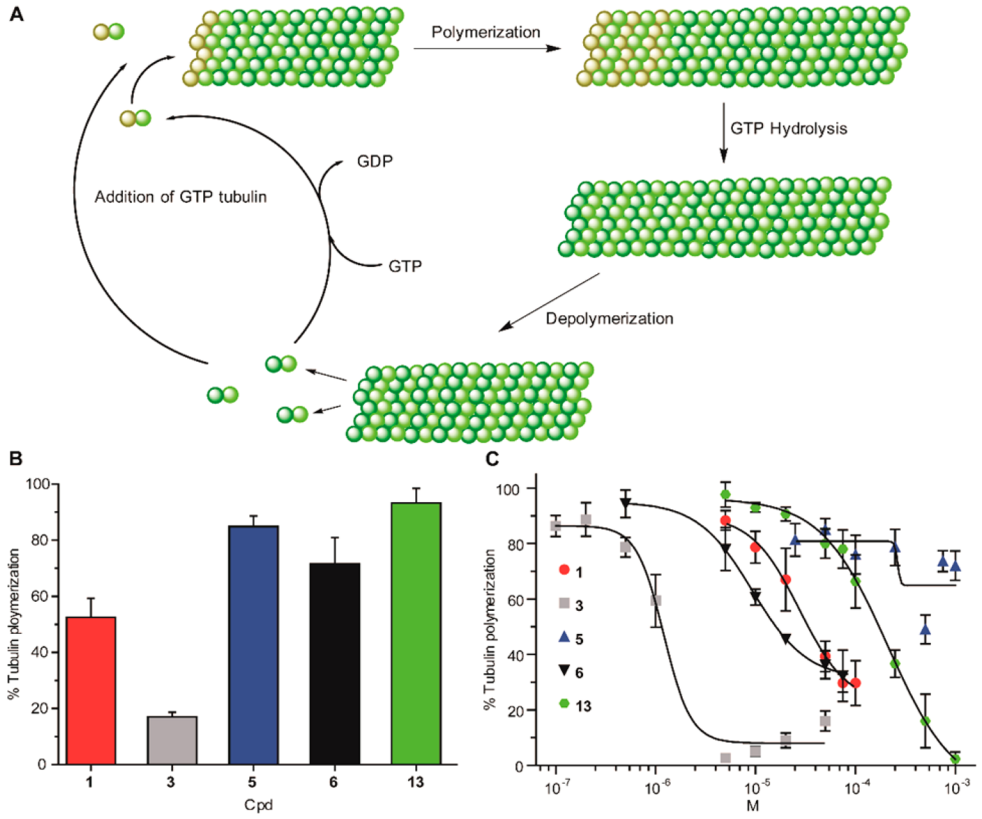

Figure 5. (A) Schematic representation of microtubule polymerization. (B) Quantification of the effect of 50 μM **1**, **3**, **5**, **6**, and **13** on microtubule polymerization. (C) Dose–response curves of **1**, **3**, **6**, and **13** on microtubule polymerization *in vitro*. Derivative **5** did not show an effect on the tubulin polymerization up to 1 mM. For B and C, an average of three independent experiments and standard deviations are shown. For detailed information, see the Supporting Information.

DISCUSSION AND CONCLUSION

Using BTB-1 as a lead compound, we synthesized derivatives **2**–**21** in one or two steps starting from commercially available building blocks. The described synthesis route allowed the robust and cost-efficient assembly of a small scale compound collection. IC_{50} studies identified several BTB-1 derivatives that potently inhibited the ATPase activity of Kif18A in the low micromolar range.

SAR studies of identically substituted sulfone (**3** and **13**) and sulfoxide (**4** and **14**) derivatives highlight the importance of the sulfone functionality for the inhibitory activity of the compounds against Kif18A. Consistently, replacing the sulfone linker of **1** with an ether linkage (**21**) resulted in an almost complete loss of inhibitory activity (Figure 6A). Further SAR studies revealed that the introduction of either electron withdrawing (**19** and **20**) or donating (**10**–**12**, **15**–**18**) substituents in the *para* position to the linker at phenyl moiety II was not tolerated. Similarly, expanding the sterical demand of phenyl moiety II by replacing it with naphthalene (**8**) resulted in a complete loss of activity (Figure 6A). Within phenyl moiety I, shifting the NO_2 group from the *ortho* (**1**) to *meta* (**2**) position to the sulfone linker caused compound inactivity, while replacing chloride (**1**) at R^1 with hydrogen (**13**) or different electron withdrawing groups like fluoride (**5**), NO_2 (**3**), or CF_3 (**6**) had no drastic effect on compound activity (Figure 6A). Unfortunately, the most potent derivatives **5** and **13** did not interfere with the localization of Kif18A to the plus ends of microtubules in mitotic cells, suggesting that treatment with these derivatives did not result in efficient Kif18A inhibition. While we cannot formally exclude the possibility that **5** and **13** are not membrane permeable, the fact that the structurally related compounds **1** and **6** induced cellular effects argues against this idea. Possibly, post-translational modifications of Kif18A in cells or its association with binding partners render Kif18A resistant to the action of **5** and **13**. Notably, **1** and **6** caused a cellular phenotype reminiscent of low doses of Nocodazole and *in vitro* studies confirmed that these compounds potently inhibited microtubule polymerization. Since microtubule dynamics affect the accumulation of Kif18A to the plus ends of microtubules,[7] it is difficult to determine if altered Kif18A localization in cells treated with **1** or **6** is a direct effect of Kif18A inhibition or indirectly caused by the undesired effect on microtubule dynamics. Furthermore, our *in vitro* microtubule polymerization assays revealed that the high cytotoxicity of **3** is likely to be mediated by its severe effect on microtubule polymerization. These data suggest that the introduction of sterically demanding electron withdrawing groups at R^1 like NO_2 (**3**) or CF_3 (**6**) shift the inhibitory activity towards microtubules, whereas small substituents like hydrogen (**13**) or fluoride (**5**) influence the activity in favor of Kif18A inhibition (Figure 6B).

In summary, we reported herein the design, synthesis, and biological evaluation of a BTB-1 analog library. We identified several novel derivatives that potently inhibited the ATPase activity of Kif18A. Most importantly, our SAR analysis enabled us to separate the undesired effect on microtubule polymerization from the aimed inhibition of Kif18A. These insights provide an important guideline for the future design and synthesis of specific and bioactive Kif18A inhibitors. Such

dx.doi.org/10.1021/cb500789h | *ACS Chem. Biol.* XXXX, XXX, XXX–XXX

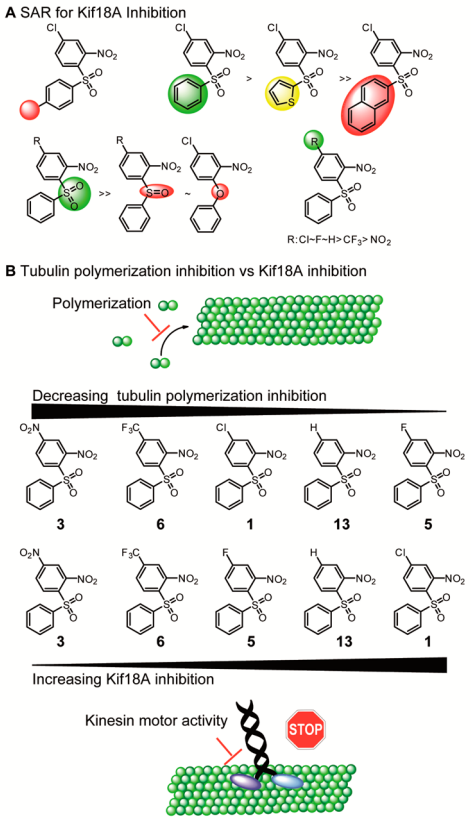

Figure 6. (A) Scheme of SAR for Kif18A inhibition. Green colored groups are essential for activity. Yellow groups are tolerated but cause some activity loss. Red groups are not tolerated and cause a complete loss of inhibitory activity. (B) The upper panel shows molecules sorted based on their inhibitory effect on microtubule polymerization, decreasing activity from left to right. In the lower panel, compounds are sorted based on their inhibitory activity towards Kif18A with the most potent compound **1** shown on the right side.

compounds would not only be invaluable tools for basic research but have the potential to open up new strategies in the treatment of mitosis-related diseases such as Kif18A over-expressing tumors.

METHODS

Full experimental details are given in the Supporting Information.

ASSOCIATED CONTENT

Supporting Information

Detailed synthetic procedures of all compounds and biological assays are available. This material is available free of charge via the Internet at http://pubs.acs.org.

AUTHOR INFORMATION

Corresponding Author

*E-mail: Thomas.U.Mayer@uni-konstanz.de.

Author Contributions

[§]These authors contributed equally.

Notes

The authors declare no competing financial interest.

ACKNOWLEDGMENTS

We gratefully acknowledge funding by the SFB 969 "Chemical and Biological Principles of Cellular Proteostasis" of the German Research Foundation (DFG) and scientific support by the Konstanz Research School Chemical Biology (KoRS-CB). We thank the Bioimaging Center (BIC) and NMR facility of the University of Konstanz for technical support.

REFERENCES

(1) Wittmann, T., Hyman, A., and Desai, A. (2001) The spindle: a dynamic assembly of microtubules and motors. *Nat. Cell Biol. 3*, E28–34.

(2) Cross, R. A., and McAinsh, A. (2014) Prime movers: the mechanochemistry of mitotic kinesins. *Nat. Rev. Mol. Cell Biol. 15*, 257–271.

(3) Welburn, J. P. (2013) The molecular basis for kinesin functional specificity during mitosis. *Cytoskeleton (Hoboken) 70*, 476–493.

(4) Mayr, M. I., Hummer, S., Bormann, J., Gruner, T., Adio, S., Woehlke, G., and Mayer, T. U. (2007) The human kinesin Kif18A is a motile microtubule depolymerase essential for chromosome congression. *Curr. Biol. 17*, 488–498.

(5) Mayr, M. I., Storch, M., Howard, J., and Mayer, T. U. (2011) A non-motor microtubule binding site is essential for the high processivity and mitotic function of kinesin-8 Kif18A. *PLoS One 6*, e27471.

(6) Weaver, L. N., Ems-McClung, S. C., Stout, J. R., LeBlanc, C., Shaw, S. L., Gardner, M. K., and Walczak, C. E. (2011) Kif18A uses a microtubule binding site in the tail for plus-end localization and spindle length regulation. *Curr. Biol. 21*, 1500–1506.

(7) Stumpff, J., Du, Y., English, C. A., Maliga, Z., Wagenbach, M., Asbury, C. L., Wordeman, L., and Ohi, R. (2011) A tethering mechanism controls the processivity and kinetochore-microtubule plus-end enrichment of the kinesin-8 Kif18A. *Mol. Cell 43*, 764–775.

(8) Stumpff, J., von Dassow, G., Wagenbach, M., Asbury, C., and Wordeman, L. (2008) The kinesin-8 motor Kif18A suppresses kinetochore movements to control mitotic chromosome alignment. *Dev. Cell 14*, 252–262.

(9) Du, Y., English, C. A., and Ohi, R. (2010) The kinesin-8 Kif18A dampens microtubule plus-end dynamics. *Curr. Biol. 20*, 374–380.

(10) Zhang, C., Zhu, C., Chen, H., Li, L., Guo, L., Jiang, W., and Lu, S. H. (2010) Kif18A is involved in human breast carcinogenesis. *Carcinogenesis 31*, 1676–1684.

(11) Nagahara, M., Nishida, N., Iwatsuki, M., Ishimaru, S., Mimori, K., Tanaka, F., Nakagawa, T., Sato, T., Sugihara, K., Hoon, D. S., and Mori, M. (2011) Kinesin 18A expression: clinical relevance to colorectal cancer progression. *Int. J. Cancer 129*, 2543–2552.

(12) Rath, O., and Kozielski, F. (2012) Kinesins and cancer. *Nat. Rev. Cancer 12*, 527–539.

(13) Catarinella, M., Gruner, T., Strittmatter, T., Marx, A., and Mayer, T. U. (2009) BTB-1: A Small Molecule Inhibitor of the Mitotic Motor Protein Kif18A. *Angew. Chem., Int. Ed. 48*, 9072–9076.

(14) Grundon, M. F., Johnston, B. T., and Matier, W. L. (1966) Proximity effects in diaryl derivatives. Part IV. Base-catalysed reactions of 2,2[prime or minute]-di(hydroxyamino)diaryl sulphones and of 2-(hydroxyamino)aryl phenyl sulphones. *J. Chem. Soc. B*, 260–266.

(15) Parveen, S., Khan, M. O. F., Austin, S. E., Croft, S. L., Yardley, V., Rock, P., and Douglas, K. T. (2005) Antitrypanosomal, Antileishmanial, and Antimalarial Activities of Quaternary Arylalkylammonium 2-Amino-4-Chlorophenyl Phenyl Sulfides, a New Class of Trypanothione Reductase Inhibitor, and of N-Acyl Derivatives of 2-Amino-4-Chlorophenyl Phenyl Sulfide. *J. Med. Chem. 48*, 8087–8097.

(16) Moore, W. J., Kern, J. C., Bhat, R., Commons, T. J., Fukayama, S., Goljer, I., Krishnamurthy, G., Magolda, R. L., Nogle, L., Pitts, K., Stauffer, B., Trybulski, E. J., Welmaker, G. S., Wilson, M., and Bodine, P. V. N. (2008) Modulation of Wnt Signaling Through Inhibition of Secreted Frizzled-Related Protein I (sFRP-1) with N-Substituted Piperidinyl Diphenylsulfonyl Sulfonamides†. *J. Med. Chem. 52*, 105–116.

(17) Wang, C., Ma, Z., Sun, X.-L., Gao, Y., Guo, Y.-H., Tang, Y., and Shi, L.-P. (2006) Synthesis and Characterization of Titanium(IV) Complexes Bearing Monoanionic [O-NX] (X = O, S, Se) Tridentate

Ligands and Their Behaviors in Ethylene Homo- and Copolymerizaton with 1-Hexene. *Organometallics 25*, 3259−3266.
(18) Huang, T. G., and Hackney, D. D. (1994) Drosophila kinesin minimal motor domain expressed in Escherichia coli. Purification and kinetic characterization. *J. Biol. Chem. 269*, 16493−16501.
(19) Hamid, R., Rotshteyn, Y., Rabadi, L., Parikh, R., and Bullock, P. (2004) Comparison of alamar blue and MTT assays for high throughput screening. *Toxicol. In Vitro 18*, 703−710.
(20) Häfner, J., Mayr, M. I., Möckel, M. M., and Mayer, T. U. (2014) Pre-anaphase chromosome oscillations are regulated by the antagonistic activities of Cdk1 and PP1 on Kif18A. *Nat. Commun. 5*, 4397.
(21) Hamel, E. (2003) Evaluation of antimitotic agents by quantitative comparisons of their effects on the polymerization of purified tubulin. *Cell Biochem. Biophys. 38*, 1−22.
(22) Dong, H., Li, Y. Z., and Hu, W. (2004) Analysis of purified tubulin in high concentration of glutamate for application in high throughput screening for microtubule-stabilizing agents. *Assay Drug Dev. Technol. 2*, 621−628.